J Comput Neurosci
DOI 10.1007/s10827-007-0021-2

Self-influencing synaptic plasticity: Recurrent changes of synaptic weights can lead to specific functional properties

Minija Tamosiunaite · Bernd Porr · Florentin Wörgötter

Received: 24 June 2006 / Revised: 21 December 2006 / Accepted: 10 January 2007

Abstract Recent experimental results suggest that dendritic and back-propagating spikes can influence synaptic plasticity in different ways (Holthoff, 2004; Holthoff et al., 2005). In this study we investigate how these signals could interact at dendrites in space and time leading to changing plasticity properties at local synapse clusters. Similar to a previous study (Saudargiene et al., 2004) we employ a differential Hebbian learning rule to emulate spike-timing dependent plasticity and investigate how the interaction of dendritic and back-propagating spikes, as the post-synaptic signals, could influence plasticity. Specifically, we will show that local synaptic plasticity driven by spatially confined dendritic spikes can lead to the emergence of synaptic clusters with different properties. If one of these clusters can drive the neuron into spiking, plasticity may change and the now arising global influence of a back-propagating spike can lead to a further segregation of the clusters and possibly the dying-off of some of them leading to more functional specificity. These results suggest that through plasticity being a spatial and temporal local process, the computational properties of dendrites or complete neurons can be substantially augmented.

Keywords Spike-timing-dependent plasticity · Dendritic spike · Back-propagating spike · Local learning

Action Editor: Wulfram Gerstner

M. Tamosiunaite
Department of Psychology, University of Stirling, Stirling FK9 4LA, Scotland

M. Tamosiunaite
Department of Informatics, Vytautas Magnus University, Kaunas, Lithuania
e-mail: minija_tamosiunaite@fc.vdu.lt

B. Porr
Department of Electronics & Electrical Engineering, University of Glasgow, Glasgow, GT12 8LT, Scotland
e-mail: B.Porr@elec.gla.ac.uk

F. Wörgötter (✉)
Bernstein Center for Computational Neuroscience, University of Göttingen, Bunsenstr. 10 (at the MPI), D-37073 Göttingen Germany
e-mail: worgott@bccn-goettingen.de

Introduction

There is growing evidence that synaptic plasticity changes during learning. Plasticity seems to be a rather dynamic process where the *history* of pre- and post-synaptic events determines the form of plasticity. This is partially reflected in the phenomenon of spike-timing-dependent-plasticity (STDP, Magee and Johnston, 1997; Markram et al., 1997), which goes one step further than classical Hebbian learning (Hebb, 1949; Bliss and Gardner-Edwin, 1973; Malenka and Nicoll, 1999; Bi and Poo, 2001) and takes into account the order of pre- or post-synaptic events: A pre-synaptic event that is followed by a post-synaptic event, will lead to long term potentiation (LTP). If the order is reversed, causality cannot have existed and long term depression (LTD) is found (Bi and Poo, 2001).

Spike timing dependent plasticity can be modeled by a *static* wavelet shaped function (for a review see Kempter et al., 1999). By contrast here we are going to use *dynamic* STDP learning curve which is calculated from the shapes of the pre- and post-synaptic potentials (Porr and Wörgötter, 2003; Saudargiene et al., 2004). Thus, in this study the shapes and timings of pre- and post-synaptic events crucially determine synaptic plasticity which is continuously changing during learning. For example, usually through the synaptic activity at a cluster of synapses the post-synaptic spike

will be triggered. This signal can then travel retrogradely into the dendrite (as a so-called back-propagating- or BP-spike, Golding et al., 2001), leading to a depolarization at this and other clusters of synapses by which their plasticity will be influenced. More locally, something similar can happen if a cluster of synapses is able to elicit a dendritic spike (D-spike, Golding et al., 2002; Larkum et al., 2001), which may not travel far, but which certainly leads to a local depolarization "under" these and adjacent synapses, triggering synaptic plasticity of one kind or another. Such local plasticity processes, predicted by theory (Saudargiene et al., 2004, 2005b), have indeed been recently confirmed in electrophysiological experiments (Froemke et al., 2005). Hence synaptic plasticity is often, if not always, to some degree influenced by the history of numerous pre- and post-synaptic events and by the location of the synapse.

In this study, we will investigate how the temporal relation between dendritic- and back-propagating spikes could influence plasticity. We will introduce a setup leading to changing learning characteristics in spatially distributed dendrites and we will show that this way useful functional properties can arise also quantifying the robustness of the observed effects. Specifically, we will demonstrate that a self-generated winner-take-all mechanism can arise from synaptic plasticity that changes over time. It appears evident that recurrent processes will influence plasticity, but so far direct experimental support for this is missing. Hence, this study attempts to assess possible consequences of such mechanisms from the theoretical side. However, we note that we do not attempt to be exhaustive with respect of the possible effects that could occur with such recurrent or spatially separated plasticity mechanisms. Instead we are focusing on a predesigned scenario to demonstrate for the first time possible functional consequences of such self-influencing plasticity mechanisms. While recent results have confirmed that synaptic plasticity can be a spatially local process (Froemke et al., 2005), the results of the current study predict that in a similar way also temporally local synaptic processes should be found at the neurons.

To this end, we will be assuming a *basic chain of events* to elicit plasticity at our model neuron. Normally a pre-synaptic spike will lead to some kind of small post-synaptic depolarization, usually an EPSP. Let us furthermore assume that through temporal and spatial summation at a cluster of synapses these EPSPs can lead to a dendritic spike (D-spike Golding et al., 2002; Gasparini et al., 2004), which represents a stronger depolarizing signal. Ideally, in this case pre- and post-synaptic events are temporally closely coupled with often not much more than 1 ms delay. Groups (bursts) of dendritic spikes will, in turn, be strong enough to drive the soma of the neuron into spiking (Golding and Spruston, 1998; Williams and Stuart, 2003). As a consequence, a back-propagating spike will be elicited and will travel retrogradely into the dendrite (Golding et al., 2001; Williams and Stuart, 2003). Such a BP-spike occurs normally clearly later, but not by much, than the pre-synaptic events which have triggered this chain.

First we note that for many neurons this chain of events may remain incomplete. Some will not produce D- or BP-spikes, for others the BP-spike might not travel very far into the dendrite (Stuart et al., 1997), not affecting more distal synapses (Sjöström and Häusser, 2006; Letzkus et al., 2006). These cases will be discussed later. For now we will assume that this event-chain shall be complete.

As a consequence of the complex dendritic structure, of most vertebrate neurons, these events can take place at different parts of the dendrite without any causal relation between them (Polsky et al., 2004). Thus, D-spikes and BP-spikes will to some degree create cross-talk at synapse clusters from which they have not originated and this cross-talk will bring signals which are not causally related to each other into interaction.

The central questions of this study are: How would this cross-talk affect synaptic plasticity at the different sites? Can useful functional properties arise from this and how are they expressed? And are the observed effects robust with respect to the model assumptions and against parameter changes?

Methods

The central assumption of this study is that different post-synaptic signals (D- vs. BP-spikes) can lead to different types of unsupervised (hebbian) learning (Froemke et al., 2005; Letzkus et al., 2006; Sjöström and Häusser, 2006). This type of learning requires an initial spatio-temporal bias from which it can extract relevant correlations. To provide this, in general, we assume that there are groups of differently strong correlated input spikes available to a neuron. This assumption is supported, for example, by the fact that the anatomical development of the nervous system preserves neighborhood relations so that spatial correlations will always exist (e.g. topographic maps (see Swindale (1996)). The goal of this study is to show how a system might continue to develop from such an initial condition. Especially we will investigate what happens when D- and BP-spikes, initially driven by weakly correlated inputs, "mix" at a synapse influencing plasticity in specific ways.

Therefore we will first introduce our synapse model before we describe the more complex full setup of the modeled circuit.

Synapse and learning rule

Figure 1 shows the synapse model we are using. It consists of AMPA as well as NMDA influences. The AMPA influence,

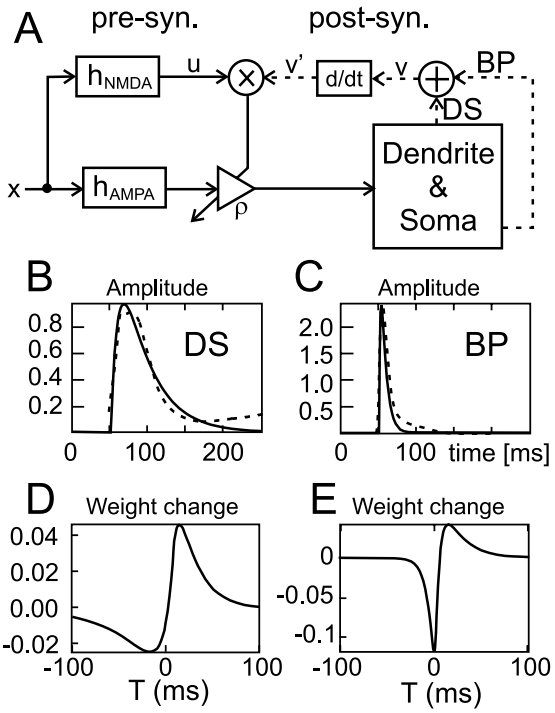

Fig. 1 The synapse model (A) and examples of D- and BP-spikes (B,C) abbreviated with DS and BP, respectively. Other symbols are: ρ, synaptic weight; x, input spike train; u, pre-synaptic signal; and v, post-synaptic signal. The plus represents a summation node, the cross denotes a multiplication (correlation), d/dt is the temporal derivative and the amplifier symbol denotes a changeable synapse ρ. (B) D-spike with $\tau = 235$ ms. (C) BP-spike with $\tau = 40$ ms, In (B) and (C) dashed is superimposed a D- and a BP-spike taken Larkum et al. (2001). (D) STDP curve obtained with the model D-spike, (E) STDP curve from the model BP-spike

does not enter plasticity, but is used to drive the soma. The NMDA influence is used as the pre-synaptic part of our learning rule.

The post-synaptic part consists of the sum of two possible influences, namely D-spikes plus BP-spikes, which arise from dendrite or soma, respectively. Note, in many cases only one (D *or* BP) of the two influences will be active at a synapse (Sjöström and Häusser, 2006; Letzkus et al., 2006, see also commentary by Bender and Feldman (2006)) Detailed equations for the pre- and post-synaptic signals will be given below.

Spike timing dependent plasticity is the pattern of learning analyzed in this study and is implemented using a differential Hebbian learning rule (Porr and Wörgötter, 2003; Saudargiene et al., 2004):

$$\frac{d\rho}{dt} = \mu u_{NMDA}(t)\dot{v}(t) \tag{1}$$

where ρ denotes the synaptic weight of a synapse, μ the learning rate and $\dot{v}(t)$ is the temporal derivative of the conjoint post-synaptic influences. Note, since we are interested in local vs. global influences we assume dendritic spikes from different dendritic branches represent local processes and do not influence each other. Back-propagating spikes, on the other hand, reach all synapses in this model and thereby represent a global influence.

The learning rule was implemented using the Euler method for numerical integration with a time step of 1 ms. Learning rate μ was varied between 0.09 and 1.5.

Panels (B-E) of Fig. 1 show typical examples of D- and BP-spikes and the weight change curves derived from them. Note, a detailed analysis for example of how AMPA and NMDA influences as well as other intrinsic parameters may modify an STDP learning window is given in our older works (Saudargiene et al., 2004, 2005a,b). Real D- and BP-spike examples taken from the literature are depicted by the dashed curves, which demonstrates the similarity of the modeled to the real signals. Evidently, D- and BP-spikes lead to differently shaped weight change curves. Specifically, and as shown previously (Saudargiene et al., 2004), an output $v(t)$ with a shallow rising flank will predominantly lead to LTP, while one with a steep rising flank results in STDP.

The main question of this study is: How will synaptic weights change if during the development of a given synapse the weight change curve itself changes? To address this question we need to introduce the full model and its equations next.

Circuit model

The model analyzed here follows the tradition of "electrically-equivalent circuit models" in physiology often employed to model neuronal channel characteristics, but in our context it is an abstraction of a real neuron including several clusters of synapses on its dendritic branches. We model AMPA and NMDA receptor activation signals (Koch, 1999), dendritic spikes initiated by inputs to the synaptic clusters (Golding et al., 2002; Larkum et al., 2001), and the back propagating spikes (Golding et al., 2001) originating after the cell has fired.

A block diagram of the model is shown in Fig. 2. Dendritic spikes are elicited following the summation of several AMPA signals passing threshold q_1. NMDA receptor influence on dendritic spike generation was not considered as the contribution of NMDA potentials to the total membrane potential is substantially smaller than that of AMPA channels at a mixed synapse.

Each synaptic cluster is limited to generating one dendritic spike from one arriving pulse group. Cell firing is not explicitly modeled but said to be achieved when the summation of several dendritic spikes at the cell soma has passed threshold q_2. This leads to a BP-spike. Progression of signals along a dendrite is also not modeled explicitly, but expressed by means of delays. Since we do not model biophysical

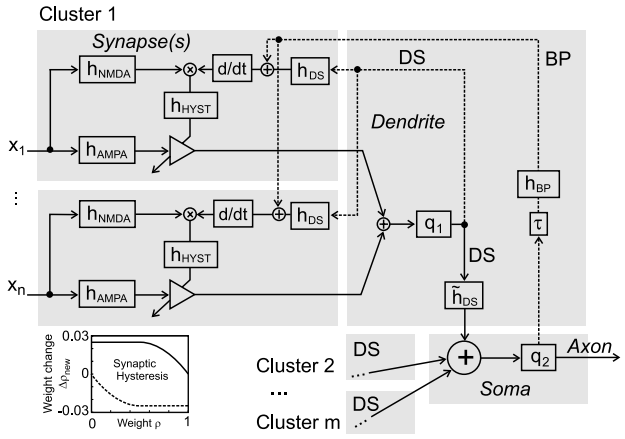

Fig. 2 Basic learning scheme with $x_1, \ldots, x_n$ representing inputs to cluster 1, h_{AMPA}, h_{NMDA} - filters shaping AMPA and NMDA signals, $h_{DS}, \tilde{h}_{DS}, h_{BP}$ - filters shaping D and BP-spikes, h_{HYST} - hysteresis type weight saturation function (see inset down left, calculated by Eq. (6) using $\Delta\rho = 0.1$), q_1, q_2 - differential thresholds, τ - a delay. Only the first of m clusters is shown explicitly; clusters $2, 3, \ldots, m$ would be employing the same BP-spike (not shown). The symbol $\oplus$ represents a summation node and $\otimes$ multiplication

processes, all signal *shapes* are obtained by appropriate filters (see below). D- and BP-spikes are of an all-or-none type.

As shape and timing interplay is the most important aspect of this study, we provide realistic timing in milliseconds for the employed signals. Absolute signal amplitudes are irrelevant and only arbitrary units are used here. Furthermore, most of the computational experiments are performed with small number of synapses in comparison to realistic synaptic convergence to save simulation time. Some, however, use large numbers, to check the validity of the other results.

Model equations

We define:

$$u_{NMDA}(t) = x(t) * h_{NMDA}(t), \qquad u_{AMPA}(t) = x(t) * h_{AMPA}(t) \tag{2}$$

where $x(t)$ is a spike train given in the usual way as a sequence of δ-functions. Note, all functions $h(t)$ are a filter functions defined in the section on Signal Shapes below. The "*" denotes a convolution.

Furthermore we define a local dendritic-summation process with:

$$y(t) = \sum_j \rho_j u_{j,AMPA}(t) \tag{3}$$

where we sum over all synaptic inputs j.

We elicit a D-spike if this process exceeds a certain threshold q_1, hence if at time-points t_i we get $y(t_i) > q_1$ we elicit a D-spike v_{DS} with:

$$v_{DS}(t) = \delta(t - t_i) * h_{DS}(t) \tag{4}$$

where $h_{DS}(t)$ is a filter shape for a D-spike. Note, we assume that pulse groups remain temporally separate such that D-spikes will not follow each other closely.

In a similar way, at the soma a BP-spike $v_{BP}(t)$ will be elicited if the signals that arrive at the soma exceed threshold q_2. In the context of this study, we assume that this happens as a consequence of one or more D-spikes arriving at the soma. Smaller somatic AMPA (or NMDA-) inputs are not considered, but could be built in in a similar way. Hence, if at time-point t_i we find that $\sum_k v^k_{DS}(t_i) > q_2$, where k is the number of clusters, then we elicit a BP-spike v_{BP} with:

$$v_{BP}(t) = \delta(t - t_i) * h_{BP}(t) \tag{5}$$

Synaptic saturation

Weights were kept in the interval [0,1] using a hysteresis type saturation function (inset at bottom of Fig. 2). The saturation was achieved applying a weight-dependent nonlinear transformation for the weight modification term $\Delta\rho$ obtained in one integration step of Eq. (1). If the weights were increasing towards one, or decreasing towards zero, the following function was applied to the weight change $\Delta\rho$:

$$\Delta\rho_{new} = \frac{1}{1 + \frac{1-\rho}{\rho}\exp(-\Delta\rho)} - \rho \tag{6}$$

The opposite cases, which capture growth of small weights and decrease of big weights, were kept linear. The transition between linear and hysteresis-saturated parts was placed at a weight value of $\rho = 0.5$. In the linear part weight modification $\Delta\rho$ was multiplied by a constant: $\Delta\rho_{new} = 0.25\Delta\rho$, to keep the derivative at the boundary between linear and nonlinear parts smooth.

It is known that in real systems some weight stabilization mechanism is employed to keep weights from excessive saturation (Bi and Poo, 1998), yet we did not employ such mechanisms in our study.

Instead the experiments were performed up the point where weights stayed in the interval [0.1, 0.9]. In Fig. 8 we will discuss that in this range saturation still does not distort the results.

Signal shapes

Filter shapes forming AMPA and NMDA channel responses, as well as back-propagating spikes and dendritic spikes used

in this study were described by:

$$h(t) = \frac{e^{-2\pi t/\tau} - e^{-8\pi t/\tau}}{6\pi/\tau} \tag{7}$$

with $h(t) = 0$ for $t < 0$, where τ determines the total duration of the pulse. The ratio between rise and fall time is 1:4. Parameter for the standard signals were adapted from textbooks (Koch, 1999), other obtained from own curve fitting with real DS- and BP-spikes (e.g. see Fig. 1. Hence, for modeling the AMPA channel potentials (h_{AMPA}) a filter with $\tau_A = 6$ ms was used, for modeling the NMDA channel potentials (h_{NMDA}) we use $\tau_N = 120$ ms, for dendritic spikes (h_{DS}) we set $\tau_{ds} = 235$ ms and for back-propagating spikes (h_{BP}) a filter with $\tau_{bp} = 40$ ms is employed. As described above, AMPA signals were employed for initializing dendritic spikes, NMDA signals were used as inputs $u(t)$ to the learning rule, and dendritic spikes, and the back-propagating spikes were used as outputs $v(t)$ for the learning rule.

Note, in this study, we have approximated the NMDA characteristic by a non-voltage dependent filter function. In conjunction with STDP, this simplification is justified by the analytical solutions for STDP curves derived in Saudargiene et al. (2005a), which show that voltage dependency induces only a second-order effect on the shape of the STDP curve and is confirmed by the similarity of the curves in the current study (Fig. 1(D) and (E)) to those obtained with a more complete model used in our older studies (compare to Fig. 5 in Saudargiene et al. (2004)). This approximation leads to a gain in simulation speed particular for simulations with several 100 synapses.

Results

Analytical integration of the learning rule for interacting D- and BP-spikes

In local synaptic growth when only a dendritic spike is present the STDP window is obtained by integrating the learning Eq. (1) over time:

$$\begin{aligned}\Delta\rho(T) &= \int_{-\infty}^{\infty} u_{NMDA}(t)\dot{v}(t)\,dt \\ &= \int_{-\infty}^{\infty} h_{NMDA}(t+T)\frac{d}{dt}h_{DS}(t)\,dt \\ &= \begin{cases} \int_{0}^{\infty} h_{NMDA}(t+T)\frac{d}{dt}h_{DS}(t)\,dt & \text{if } T > 0 \\ \int_{-T}^{\infty} h_{NMDA}(t+T)\frac{d}{dt}h_{DS}(t)\,dt & \text{if } T \le 0 \end{cases}\end{aligned} \tag{8}$$

where T is a time shift of the input in respect to the dendritic spike. Hence in the following it is important to remember that we *always* use the occurrence of the D-spike, which is the first possibly occurring post-synaptic signal, as our zero time-point! Note, furthermore, that these equations assume single signals, hence we do not treat multiplets of inputs here.

After integration one obtains:

$$\Delta\rho(T) = \begin{cases} \dfrac{\left(\tau_{ds}{}^2\,\tau_N{}^2\,e^{-\frac{2\pi T}{\tau_N}}\left(4\tau_{ds}+\tau_N-(\tau_{ds}+4\tau_N)\,e^{-\frac{6\pi T}{\tau_N}}\right)\right)}{12\,(\tau_{ds}+\tau_N)\,(4\tau_{ds}+\tau_N)\,(\tau_{ds}+4\tau_N)\,\pi^2} & \text{if } T > 0 \\ \dfrac{\left(\tau_{ds}{}^2\,\tau_N{}^2\,e^{\frac{8\pi T}{\tau_{ds}}}\,\pi^2\left(4\tau_{ds}+\tau_N-(\tau_{ds}+4\tau_N)\,e^{-\frac{6\pi T}{\tau_{ds}}}\right)\right)}{12\,(\tau_{ds}+\tau_N)\,(4\tau_{ds}+\tau_N)\,(\tau_{ds}+4\tau_N)\,\pi^2} & \text{if } T \le 0 \end{cases} \tag{9}$$

where τ_N is the filter parameter for the input NMDA signal, and τ_{ds} the filter parameter for the D-spike (Eq. (7)). The obtained learning window in each of the two parts is composed as a difference of two exponentials (similar to a spike itself), and has a shape with a maximum in the interval $T > 0$ and a minimum in the interval $T \le 0$. An example of this is shown in Fig. 1(D). Remember that positive values of T represent the case where the input was coming before the output and vice versa. The curve has mainly an LTP characteristic for positive shifts T, and an LTD characteristic for the negative shifts (see also Saudargiene et al. (2004, 2005a)).

Figure 1 (E) shows an STDP curve, obtained with a much sharper BP-spike, using τ_{bp} instead of τ_{ds}. Most often in this study both such post-synaptic signals will interact in time. In these cases, one finds that, as soon as a strong BP-spike occurs, the expression of the type of plasticity (LTP or LTD) will be dominated by the temporal relation between pre-synaptic signal and the BP-spike and not any more by its relation to the much weaker D-spike. Alternatively if the D-spike at a synaptic location is stronger than any other post-synaptic signal it will continue to dominate plasticity. This seems to correspond to new physiological observations concerning the relations between post-synaptic signals and the actually expressed form of plasticity (Wang et al., 2005).

We will analyze the influence of the BP-spike on the weight change $\Delta\rho$ by analyzing the function $\Delta\rho(T_{bp})$, where T_{bp} is a *relative* time shift of a BP-spike in respect to the D-spike (the zero time-point) and not relative to the pre-synaptic signal. We assume that if a cluster of synapses itself initiates the BP-spike, through the D-spike generated by this cluster, the BP-spike comes with a positive shift T_{bp} of several milliseconds. This case is important also in the sections below and we call it the "causal chain of events":

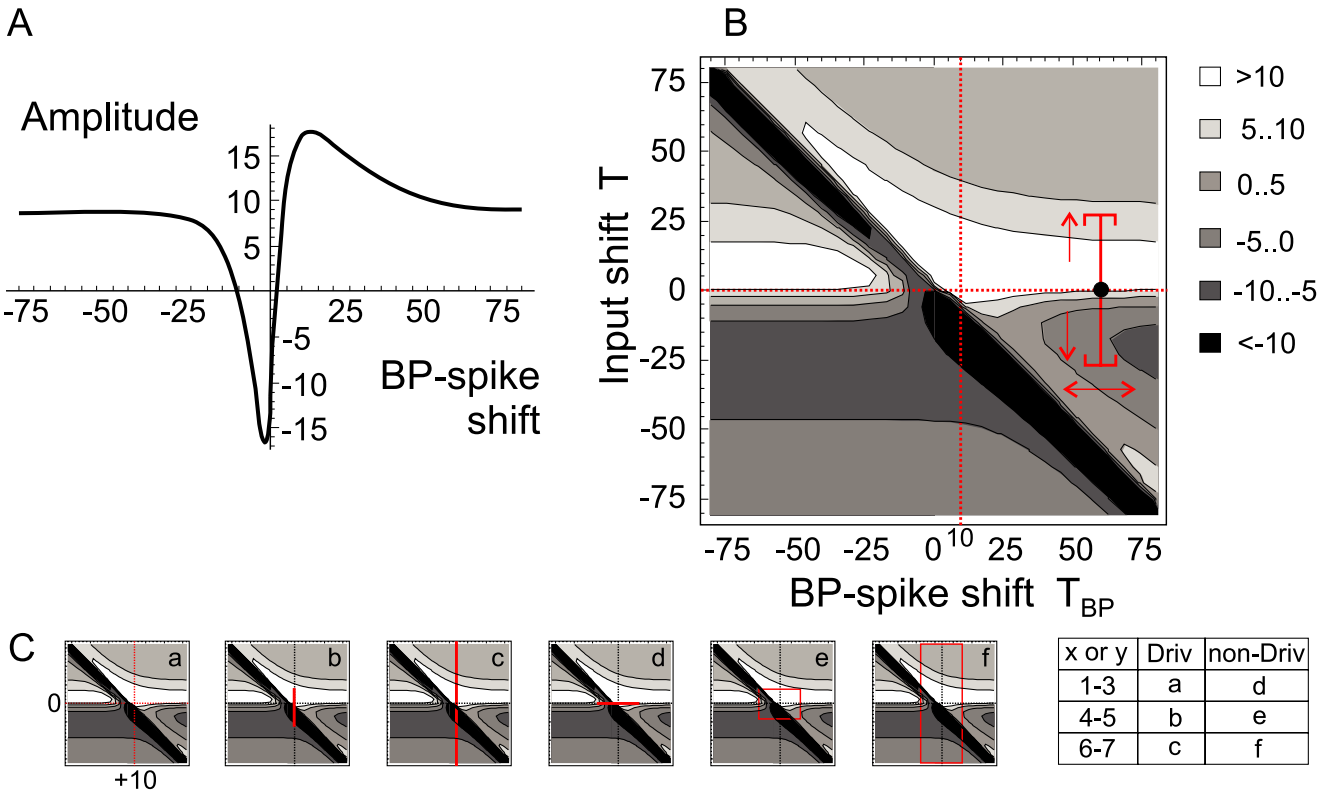

Fig. 3 Weight change dependence of a BP-spike shift: function $\Delta\rho(T_{bp})$ for $T = 0$ (A) and weight change dependence on input *and* BP-spike shifts: function $\Delta\rho(T, T_{bp})$ (B). Parameters: $A = 10$, $\tau_N = 120$; $\tau_{ds} = 235$, $\tau_{bp} = 40$, arrows will be explained in the Appendix. Panel C shows different integration windows relevant for the section on "Self-influencing plasticity"

input→D-spike→ BP-spike. Consequently for such causal cases the interval of small positive shifts is of interest in the $\Delta\rho(T_{bp})$ function. If a BP-spike is caused by another cluster, we assume that it can come at any random moment, with either a positive or a negative shift, consequently here we analyze both positive and negative shift intervals.

To get the required function we will integrate Eq. (1) from $-\infty$ to ∞ to obtain the overall weight change obtained in one learning epoch. As compared to the previous case, where we had looked only at the dendritic spike, here we are adding a BP-spike $h_{BP}(t - T_{bp})$ to the output, multiplied by an amplitude factor A. We calculate the result for the case where D-spike and inputs occur together ($T = 0$):

$$\begin{aligned}
&\Delta\rho(T_{bp}) \\
&= \int_{-\infty}^{\infty} h_{NMDA}(t)\frac{d}{dt}(Ah_{BP}(t - T_{bp}) + h_{DS}(t))dt \\
&= \begin{cases} \displaystyle\int_{0}^{\infty} h_{NMDA}(t)\frac{d}{dt}(Ah_{BP}(t - T_{bp}) + h_{DS}(t))dt \\ \qquad\qquad \text{if } T_{bp} \le 0 \\ \displaystyle\int_{T_{bp}}^{\infty} h_{NMDA}(t)\frac{d}{dt}(Ah_{BP}(t - T_{bp}) + h_{DS}(t))dt \\ \qquad\qquad \text{if } T_{bp} > 0 \end{cases}
\end{aligned} \tag{10}$$

$$\begin{aligned}
&\Delta\rho(T_{bp} \le 0) \\
&= \frac{A\,{\tau_{bp}}^2\,{\tau_N}^2\,e^{\frac{2\pi T_{bp}}{\tau_{bp}}}\left(-\tau_{bp} - 4\tau_N + (4\tau_{bp} + \tau_N)\,e^{\frac{6\pi T_{bp}}{\tau_{bp}}}\right)}{12\,(\tau_{bp} + \tau_N)\,(4\tau_{bp} + \tau_N)\,(\tau_{bp} + 4\tau_N)\,\pi^2} \\
&\quad + \frac{{\tau_{ds}}^2\,(\tau_{ds} - \tau_N)\,{\tau_N}^2}{4(\tau_{ds} + \tau_N)\,(4\tau_{ds} + \tau_N)\,(\tau_{ds} + 4\tau_N)\,\pi^2}
\end{aligned} \tag{11}$$

$$\begin{aligned}
&\Delta\rho(T_{bp} > 0) \\
&= \frac{A\,{\tau_{bp}}^2\,{\tau_N}^2\,e^{-\frac{8\pi T_{bp}}{\tau_N}}\left(-\tau_{bp} - 4\tau_N + (4\tau_{bp} + \tau_N)\,e^{\frac{6\pi T_{bp}}{\tau_N}}\right)}{12\,(\tau_{bp} + \tau_N)\,(4\tau_{bp} + \tau_N)\,(\tau_{bp} + 4\tau_N)\,\pi^2} \\
&\quad + \frac{{\tau_{ds}}^2\,(\tau_{ds} - \tau_N)\,{\tau_N}^2}{4(\tau_{ds} + \tau_N)\,(4\tau_{ds} + \tau_N)\,(\tau_{ds} + 4\tau_N)\,\pi^2}
\end{aligned} \tag{12}$$

As can be observed from the expressions the actual direction of weight change heavily depends on filter width parameters τ_N, τ_{ds}, τ_{bp}. In our experiments τ_{ds} was kept bigger than τ_N, so the second term gives a positive lift of the function. Furthermore we observe that the $\Delta\rho$ curve is composed as a difference of two exponentials, as in the previous case. The plot of the weight change curve is provided in Fig. 3(A). Since here D-spike and inputs are assumed to occur together

($T = 0$) we observe that the flat parts of the curve, where the BP-spike is too far away to exert its influence, still remain clearly above zero, which is due to the fact that the D-spike alone triggers LTP. Furthermore, one can see that the synapses for which a BP-spike comes several milliseconds later than the D-spike (causal case) will be growing most strongly. For the synapses where a BP-spike comes several milliseconds earlier than a D-spike weights will be most strongly depressed.

Releasing the constraint that the input comes together with the D-spike, expressions for the function $\Delta\rho(T, T_{bp})$ gets more complex but could still be calculated (not shown). Instead a contour plot for the resulting function, with amplitude factor for the BP-spike $A = 10$, is provided in Fig. 3(B). Weights are mainly increased when the time shift T_{bp} is bigger than $-T$. The case $T_{bp} > -T$ corresponds to the situation when the BP spike comes after the input and weights increase (upper right triangle, lighter colors), while they are decreased in the lower left triangle (dark colors). However some finer structure exists due to interplay of BP-spike and D-spike. Remember, the D-spike is assumed to be elicited at zero time point. Thus regions of opposite sign close to $T = 0$ (negative, darker in the right and positive, lighter in the left) are obtained due to the D-spike influence. The slope at the line $T_{bp} = -T$ is steep, and the behavior of the system is rather sensitive to small shifts of the BP-spike if it is close to the input spike. Note, panel A is really a horizontal cross-section at $T = 0$ through panel B.

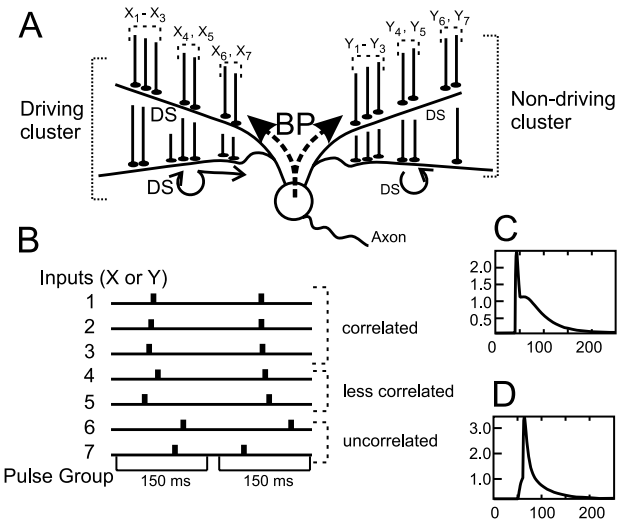

Fig. 4 (A) Model neuron with two dendritic branches (left and right), consisting of two sub-branches which get inputs X or Y, which are similar for either side. (B) Schematic diagram of the distribution of input spikes for two pulse groups. Each line carries only a single spike. Learning is performed in an adiabatic condition, where only one pulse group, will influence plasticity at the given moment. Individual input timings are drawn from a uniform distribution from within a pre-specified interval. We distinguish three basic input groups: *strongly correlated* inputs (several inputs over an interval of up to 10 ms), *less correlated* (dispersed over an interval of 10–100 ms) and *uncorrelated* (dispersed over the interval of more than 100 ms). (C,D) Mixed D- and BP-spike signals showing how signal summation arises in our model. (C) D- and BP-spikes, with $\tau = 235$ ms and $\tau = 40$ ms, time shift of the BP-spike -10 ms (acausal, BP-spike comes after D-spike), (D) the same D- and BP-spikes but with a 10 ms causal BP-spike shift

Self-influencing plasticity

The goal of the following section is to investigate into temporally changing plasticity. We will investigate a setup where

> During the learning process, at a given set of synapses plasticity is *first* dominated by the D-spike and later by a BP-spike leading to two different "phases" in the plasticity of the respective synapses.

Figure 4(A) shows how two-phase plasticity could arise from a generic setup. We can assume that inputs to large compact clusters of synapses are similar (*within* all left *or* all right branches in Fig. 4(A)) but dissimilar over larger distances (*between* left and right branches). First, e.g. early in development, synapses may be weak and only the conjoint action of many synchronous inputs will lead to a local D-spike. Local plasticity, from these few D-spikes (indicated by the circular arrow under the dendritic branches in Fig. 4), however, might strengthen these synapses and at some point a D-spike is elicited more reliably. Hence more often more than one D-spike will be elicited within a short temporal interval, (e.g. from similar inputs at the top and bottom branches from either side) and these D-spikes might sum at the soma driving the cell into spiking. As a consequence a BP-spike will be elicited and this, being of higher amplitude, might then exert a more global effect on plasticity by traveling back to (all) different synapse clusters, taking over the helm of plasticity there. In this case, however, only that cluster from which the BP-spike originated will continue to grow (causal coupling in the STDP curve), while all others might even shrink.

We emulated such a system by a simplified model system with only one left and one right branch, assuming that in the beginning the cell does not fire, and synapse development on both branches is based on dendritic spikes. Further we assume that at some point (after synapses have strengthened) the cell is driven into spiking from one of the two sides, and the BP-spikes start influencing learning.

In the next section we will quantify what happens in such a setup, when multiple inputs with different degrees of synchrony arrive.

A self-generated winner-take-all mechanism

In Fig. 5 we have simulated two clusters each with seven synapses. For both clusters, we assume that the input activity for three synapses is closely correlated and that they occur in a temporal interval of 6 ms (group x, y: $1 - 3$). Two more inputs are wider dispersed (interval of 35 ms,

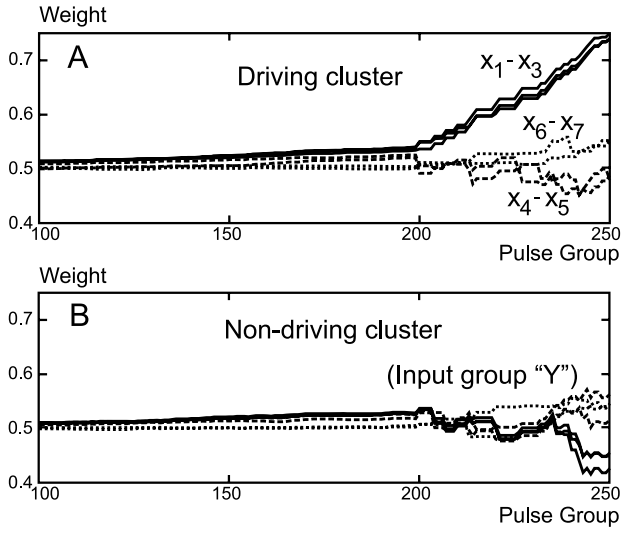

Fig. 5 Temporal weight development for the setup shown in Fig. 4 with one sub-branch for the driving cluster (A), and one for the non-driving cluster (B). Initially all weights grow gradually until the driving cluster leads to a BP-spike after 200 pulse groups. Only the weights of its group x_1-x_3 will continue to grow, now at an increased rate. Parameters: $\mu = 0.1$, BP-spike initiated 10 ms later than the driving D-spike, correlated inputs distributed over the interval of 6 ms, less correlated −35 ms, least correlated −150 ms, BP-spike/D-spike amplitude relation 4.2, shaped by Eq. (7), non-driving cluster center randomly shifted over ±20 ms interval around the driving cluster center

group x, y: 4, 5) and the two remaining ones arrive rather uncorrelated in an interval of 150 ms (group x, y: 6, 7). The notion of clustered synapses is to a great extent discussed in Govindarajan et al. (2006) supporting our assumptions. In all experiments, inputs are uniformly distributed within their respective intervals. Hence each pulse group was 150 ms long, where a complete pulse group determined by the above parameters was elicited. The activity of the second cluster is determined by the same parameters. Pulse groups arriving at the second cluster, however, were randomly shifted by maximally ±20 ms relative to the center of the pulse group of the first cluster.

All synapses start with weights 0.5 (medium), which will not suffice to drive the soma of the cell into spiking. Hence in the beginning plasticity can only take place by D-spikes. As mentioned before, we assume that D-spikes will not reach the other cluster. Hence, learning is local. The small initial weights also lead to the fact that at the beginning of learning more inputs (roughly four within an interval of 4 ms) need to arrive synchronously to elicit a D-spike than later.

The wide D-spikes will lead to a broad STDP-like learning curve, employing a span of the curve about ±20 ms around zero, that covers the dispersion of input groups 1–3 as well as 4, 5. Furthermore it has a significantly bigger area under the LTP part as compared to the LTD part at that span. As a consequence, in both diagrams (Fig. 5(A) and (B)), up to pulse group 200) we see that *all* weights 1−5 grow, only 6, 7 remain at 0.5. The correlated group 1−3, however, benefits most strongly, because it is more likely that a D-spike will be elicited by this group (and probably one other spike) than by any other combination. Hence their pre-post firing relation remains close to the origin of the STDP curve.

Conjoint growth at a whole super-cluster of such synapses would now, as described above, at some point drive the cell into somatic firing. We emulate this for the driving cluster at time point 200 where the signal coming from its converging synapses has reached the required strength (Fig. 5(A)). In general, firing of one, but not the othe cluster is due to the fact that the input properties of the two input groups are different leading to less weight growth in the other cluster.

As soon as this happens a BP-spike is triggered and the STDP curve takes a shape similar to that in Fig. 1(E) now strongly enhancing all causally driving synapses, hence group $x_1 - x_3$ (Fig. 5(A)). This group grows at an increased rate while all other synapses, both in driving and non-driving cluster shrink.

The system described so far consists of a first, "pre-growth" phase (until the BP-spike sets in) and a second phase where only one group of synapses grows strongly.

In general this example describes a scenario where groups of synapses will alter their plasticity characteristics during learning. First they undergo less selective classical Hebbian-like growth, while later more pronounced STDP sets in selecting only the driving group.

The question arises, why a pre-growth phase would be beneficial? Cannot the same results be achieved with just the second phase? To answer this question, control simulations in a once more simplified model system with only one driving cluster, and only two pulse groups, correlated and less correlated, three synapses each, have been performed, where the BP-spike was immediately elicited. In this case, learning is much faster from the very first iterations, and as a consequence several times synapses of the less-correlated group take the lead just growing by chance more than the others in the first few pulse groups (one case of such an event is shown in Fig. 6(A)), while in the two phase case the more correlated group grows without notable disturbance from the less correlated group (Fig. 6(B)). The local and "much softer" pre-growth phase avoids unwanted noise-induced symmetry breaking by gradually separating the correlated from the less correlated synapses, before introducing a strong mechanism of final growth. Hence, with a pre-growth phase higher values of μ can be set right from the beginning, where μ will exert its true influence only after pre-growth, which is desirable because it makes learning faster. Particularly early in development, when, presumably, there is still little structure and very weak synapses in the network such a 2-phase mechanism may assure correct development.

The above obtained results from our calculations allow us to qualitatively explain the weight growth in the three different groups (correlated, less-correlated and uncorrelated).

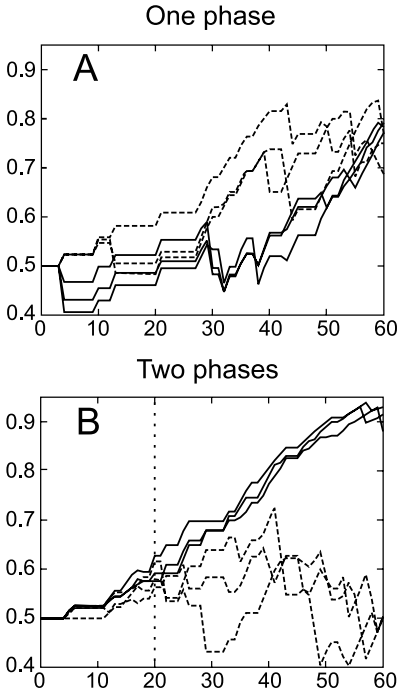

Fig. 6 Temporal weight development: (A) when the preliminary soft growth phase is absent, and (B) when it is present. Three correlated input weights—solid lines, three less correlated- dashed lines. In (B) the dotted line shows where the second phase starts. Parameters: $\mu = 1.5$, BP-spike initiated 10 ms later than the driving D-spike, correlated inputs—distributed over the interval of 9 ms, less correlated 34 ms, BP-spike/D-spike amplitude relation 4.2., shaped by Eq. (7)

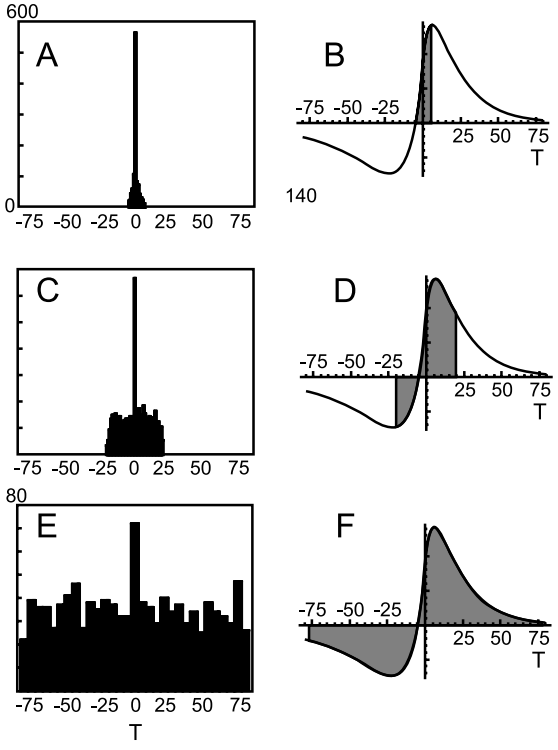

Fig. 7 Sample input-D-spike shift distributions obtained in a model run for the correlated inputs (A), less correlated (C) and uncorrelated (E). Spans of distributions of inputs on an STDP learning window (D-spike based), correlated (B), less correlated (D) and uncorrelated (F). Correlated inputs are distributed over the interval of 6 ms, less correlated - 35 ms, least correlated - 150 ms, $\mu = 0.09$, first phase 200 pulse groups, second phase 400 pulse groups, results taken beginning with the 50 pulse group to avoid the transient

D-spike without BP-spike. As before we assume that single inputs will not trigger D-spikes. Figure 7(A), (C) and (E) shows three typical distribution of D-spike times relative to the inputs of each group. The high peaks at zero reflect the case where an input had actually caused a D-spike following some pre-depolarization from other inputs. Clearly this happens most often in the correlated group. In the other two groups a much wider dispersion of D-spike times is observed.

During phase 1 (pre-growth in Fig. 5) no BP-spikes occur and we can consider the interaction of these distributions with the plain D-spike-dependent weight change curve shown in Fig. 1 and re-plotted in panels B, D, F here. The overlap between distributions and weight change curve are shaded in gray. Growth strongly dominates in the correlated group, is less expressed in the less correlated group, and in the uncorrelated group positive and negative influences are almost equal, thus only very little growth occurs. This explains the drifting apart of the curves in the pre-growth phase in Fig. 5.

D-spike and BP-spike. Once a BP-spike is triggered (phase 2) things become more complicated but we can unravel this looking at Fig. 3(B) and (C).

The six different panels in Fig. 3(C) depict over which parts of the two-dimensional curve we have to integrate in order to get the *average* effect observed in the different groups in Fig. 5. On the right side of panel C the different groups $x_1 - x_7$ and $y_1 - y_7$ of the driving and non-driving cluster are associated to the small panels labeled a–f.

Driving Cluster: For example, for the correlated group of the driving cluster the generic "causal chain of events" is that the input occurs (almost) simultaneous to the D-spike, hence $T \approx 0$ ms; and the D-spike is soon followed by a BP-spike, hence realistically at $T_{BP} \approx 5$–10 ms. This is depicted in sub-panel a, where we use the $T_{BP} = 10$ ms line because this had actually been used in the model. Thus, integration of the 2-D weight-change curve takes place most often at or very close to the cross-section of both dotted lines, which is clearly a positive domain, leading to weight-growth.

For the less-correlated groups of the driving cluster (sub-panels b,c) T_{BP} remains at the same time-point but the average integration window gets widened along the vertical line ($T \neq 0$), indicated by the red line segment, and growth and shrinkage average out.

Non-driving Cluster. For the non-driving cluster there is no relation between the moment when the BP-spike occurs to that of the cluster's D-spikes. Above we had, however,

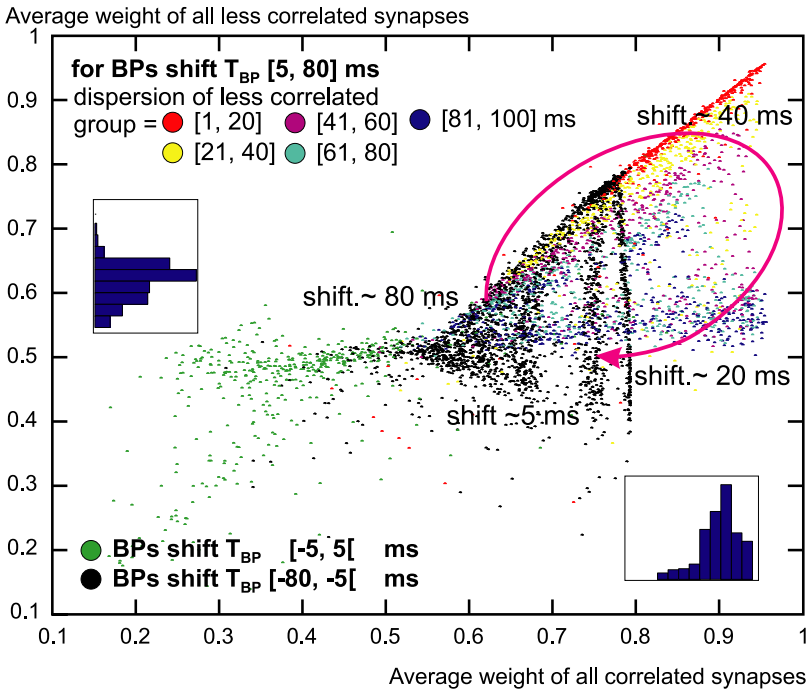

Fig. 8 Robustness of the observed effects. Plotted are the average weights of the less correlated group (ordinate) against the correlated group (abscissa). Colors depict different plasticity characteristics. Simulation with three correlated and three less correlated inputs, for AMPA $\tau = 6$ ms, for NMDA $\tau = 117$ ms, for D-spike $\tau = 235$ ms, for BP-spike $\tau = 6$–66 ms, $q_1 = 0.14$, D-/BP-spike amplitude relation from $1/1.5$ to $1/15$, depending on BP-spike width, and keeping the area under the BP-spike constant, $\mu = 0.09$, first phase 200 pulse groups, second phase 400 pulse groups. Inset histograms show the cumulative correlated and less correlated weights

described that we had on purpose restricted the center of activity of the non-driving cluster to an interval of ±20 ms with respect to the center of activity of the driving cluster. Thus, now we get an integration window of about 40 ms width centered at the BP-spike occurrence time (sub-panels d–f). The gross-effect, however is the same, synapses will on average not grow in these integration windows. In the next section we will try to show that the observed effects are also robust against parameter variations and noise.

Robustness

Figure 8 shows a color coded plot of 5000 experiments with the same basic architecture, using only one synapse cluster and the same chain of events as before but with variable parameters. Only “strong correlated" (<10 ms) and “less correlated" (10−100 ms) inputs were used in this experiment where we vary the distributions and provide an analysis. Each point represents one experiment consisting of 600 pulse groups. On the abscissa we plot the average weight of the three correlated synapses; on the ordinate the average weight of the three less correlated synapses after these 600 pulse groups. Learning rate and other parameters were chosen so as to avoid strong saturation effects (outside the weight interval $[0.1, 0.9]$). This was verified by assessing possible distortions of the distribution of the data points for correlated and less-correlated weights binning the data accordingly and plotting histograms (insets in A). These histogram show, as expected, that correlated weights on average grow more strongly than less-correlated ones, but there is no distortion visible from possible saturation effects.

Furthermore, we assume, as in the last experiment, that a BP-spike is triggered as soon as q_2 is passed, which, we suppose, happens around pulse group 200 in all cases.

Four parameters were varied to obtain this plot.

1. The width of the BP-spike was varied between roughly 5 ms and 50 ms.
2. The interval width for the maximal dispersion of the temporal distribution of the three correlated spikes was varied between 1 ms and 10 ms. Hence 1 ms amounts to three synchronously elicited spikes.
3. The interval width for the maximal dispersion of the temporal distribution of the three less correlated spikes was varied between 1 ms and 100 ms.
4. The shift of the BP-spike with respect to the beginning of the D-spike was varied in an interval of ±80 ms. Acausal cases were included because they represent the situation where the driving cluster has elicited a BP-spike which can arrive at any time at the non-driving cluster.

We will see that mainly parameters 3 and 4 have an effect on the results. The first parameter, BP spike width, shows some small interference with the spike shift for the widest spikes, but these are not causing significant effects on the results and will not be shown. The second parameter has almost no influence, because the total interval is rather small even if it is 10 ms.

Color coding is used in Fig. 8 but color transitions are arbitrary and we use coloring only to better depict the influence of parameters 3 and 4 in their different ranges. Colors “black”, “green” and “others” (all other colors) refer to a BP-spike shift T_{BP} of less than −5 ms (black), between −5 ms

and +5 ms (green) and larger than +5 ms (others). Other colors specify dispersions of the less correlated group in the region of causal (>+5 ms) BP-spike shifts T_{BP}. The region of causal BP-spike shifts considered in more details as the example of a slower and then more pronounced growth demonstrated in (Fig. 5(A)) has been drawn specifically from that region.

As the main observation of this section we state that two distinct regions (tails) can be distinguished in the figure, a diagonal and a horizontal one. If a point falls on the diagonal tail, that shows that both, the weights of the more- and those of the less correlated group, grow; while on the horizontal tail only the more correlated ones grow. This distribution confirms that there are many cases which correspond to the case shown in Fig. 5(A) (points in the horizontal tail of Fig. 8) demonstrating that the parameter range for this type of behavior is considerably large. There are, however, also many conventional situations, where both groups grow in a similar way (diagonal tail). The actual location of any data point is determined by two parameters: 1) the dispersion of the less-correlated group (relative to the correlated group) and the shift of the BP-spike. In general, one finds that with a small dispersion (colors red and yellow) data points cluster on the diagonal tail. This is due to the fact that is this case there is little difference between the correlated and less-correlated group, because their spike-dispersions are similar. However, already for the yellow group (but not yet for the red) data-points may fall onto the horizontal tail or lie in between. This happens for small BP-spike shifts (e.g. <20 ms). The limit case of a zero BP-spike shift may help to understand this: In this case spikes from the less-correlated group come very often later than the BP-spike and fall in the LTD-part of the STDP window, hence growth and shrinkage average out. Whereas spikes from the correlated group come before the BP-spike and their synapses grow. As a consequence these data-points are on the horizontal tail.

In the Appendix we provide a very detailed analysis of the complete set of data points over wider parameter ranges including learning rates, amplitudes, number of synapses, and thresholds, helping the interested reader to better understand and reproduce these results if desired.

Discussion

In the current study we have investigated how different learning rules can interact in space and time. Our study rests of the plausible suggestion that synaptic plasticity itself might not be a pre-defined, static process, but that it can change following the properties of the electrical and (not-modeled) chemical signals, which, in turn, are derived from the activity, elicited by these and other synapses, themselves. Clearly this paper cannot try to capture the true complexity of synaptic plasticity, which relies on complex cascades of enzymes and second messengers. Already in the precursor of this study (Saudargiene et al., 2004, 2005a), we had at great length discussed the shortcomings of such state-variable based modeling approaches and would like to direct the reader to these papers concerning such questions. Here we would like to address different issues.

To this end we would like to first summarize the main assumptions of our study, to give the reader also an idea about possible shortcomings of our model. All these assumption are, however, supported by the literature (as discussed throughout the text of this paper) and it appears to be a quantitative rather than a qualitative issue for a given synapse to which degree each individual prerequisite summarized here would exert its influence. We assume that (1) inputs having originated from the same source tend to terminate in a restricted area of a dendritic tree (synaptic clustering, (Govindarajan et al., 2006)); (2) inputs from the same source are correlated in time; (3) input activity passing a threshold can produce a dendritic spike; (4) dendritic spikes having originated locally in a dendrite can travel to and sum up at the soma; (5) weight change at a synapse is governed by the STDP rule, where (6) both D, and BP-spikes, or the combination of the two can play the role of an output signal; (7) BP spikes start being elicited only after weights have grown to some extent (through more reliable induction of D-spikes), (8) learning starts locally with first *only* D-spikes influencing learning and (9) continues with *both* D- and BP-spikes influencing learning; (10) BP-spikes have a shorter duration, and a bigger amplitude than D-spikes, and (11) thus produce more selective STDP learning windows; (12) inputs to a model neuron come in groups, which are spread out over time that each group can be considered separately, (13) in each group only one input spike per synapse occurs (or alternatively we consider the influence of only the first spike pair on learning).

Hence, it is obvious that the shown architectures had been specifically designed for this model. The goal of this study, however, was to show how useful computational properties can arise from such dendritic designs in a robust way. To this end, we had tried to raise confidence in the results of this study by investigating broad ranges of the parameter space, showing that the observed effects are essentially robust.

Temporal selectivity was also the topic of a study of Eurich et al. (1999) which, however, addresses the question of how to select an appropriate subset of delay lines from a range of delays in a network of neurons. By contrast, in our paper, we had focused on temporal effects showing how learning rules could change over time as the consequence of the changing synaptic properties themselves. In the chosen setup, slow synaptic growth first drives a group of synapses apart according to their intrinsic "correlatedness," then in a second phase, when a BP-spike gets elicited, these pre-sorted synapses

become finally separated and only the best-correlated group continues to grow. This two-phase process makes our approach different to that of Song et al. (2000) who had shown in a single-phase learning scenario how strengthening of a cluster of synapses might be achieved through STDP-based learning from random fluctuation of otherwise uniform input by which a better correlated cluster wins.

In this study we have been using a model setup with only one pulse on each input line during one learning trial. It is conceivable that combinations of more than on pulse on any given input line might lead to still more complex results. Yet due to the known fact that the first pairing essentially determines if LTP or LTD will occur, any following spike will have much less influence (Froemke and Dan, 2002; Wespatat et al., 2004; Shouval and Kalantziz, 2005). Thus, these physiological findings suggest, that the effects observed here using only one spike pair would hold also for multiplets, at least in a qualitative sense. To directly address multiplets one could increase the model complexity towards higher biophysical realism, where only the latest models make serious attempts to capture pulse groups, too (Abarbanel et al., 2003; Rubin et al., 2005; Yeung et al., 2004). There are, however, also simpler ways to mend this situation without having to alter the basic model structure as discussed in Saudargiene et al. (2005b).

In our model a linear D- and BP-spike combination was influencing otherwise non-linear weight-saturated learning. Such a model may interact "too soft" with respect to the interactions of D- and BP-spikes. Transitions between LTP and LTD may in reality occur more abruptly, or, once triggered, LTD (or LTP) may not be reversible through an additional later coming signal, usually through the BP-spike. Experimental results, however, are not conclusive and it remains unclear under which conditions LTD and LTP can be reversed or not (Wang et al., 2005). These questions can only be addressed with a more realistic model (Senn et al., 2000; Castellani et al., 2001; Karmarkar and Buonomano, 2002; Karmarkar et al., 2002; Abarbanel et al., 2002; Shouval et al., 2002; Abarbanel et al., 2003; Rubin et al., 2005; Yeung et al., 2004), but we believe that the core conclusions of this study, which concern influence of recursiveness and distributedness of synaptic plasticity on learning, will remain qualitatively valid even in more complex scenarios.

At the moment it is difficult to assess to what degree our conclusions will hold. There are recent results in the literature which seem to contradict our study. For example the results from Holthoff et al. (2004) and Holthoff et al. (2005), who have shown, that D-spikes will lead to a different type of plasticity than BP-spikes in layer 5 pyramidal cells in mouse cortex with single shock experiments. They have found, different from the suggestions of our study, that D-spikes will trigger mainly LTD, whereas a D-spike paired with a BP-spike will lead to LTP. This may, however, have to do with the fact that the elicited D-spikes are not strong enough to induce a large enough Calcium flux such that the low level of Ca^{2+} reached can only induce LTD. Here we have assumed that D-spikes are slow but always large enough to induce either LTP or LTD depending on their timing relation to the pre-synaptic signal, whereas this seems to be not the case in the study of Holthoff and co-workers, which would resolve the apparent conflict.

Also, it may well be that different cell types will react in a different way. For example in the hippocampus it has been shown by Golding et al. (2002) that bursts of dendritic spikes can indeed trigger LTP even if the back-propagating spike is blocked by TTX.

These and other experimental results suggest that plasticity is indeed a spatially and temporally localized process, which may lead to more complex dendritic computational properties as suggested in the current study. Especially the effect that plasticity can influence itself over the course of time appears interesting in conjunction with neural network properties.

Appendix: Detailed statistical analysis

This Appendix will provide a detailed parameter analysis of Figs. 8 and 9.

The black region of Fig. 8 (<-5 ms) shows cases of acausal BP-spike shifts $T_{BP} < 0$, that could happen at the non-driving cluster by crosstalk between clusters. In this case correlated synapses will grow to some extent, while less correlated synapses can grow or shrink. This happens because the BP-spike is too early to influence plasticity in the strongly correlated group, which will grow by the DS-mechanism only, but the BP-spike still falls in the dispersion range of the less correlated group, influencing its weights. When sub-structuring the black region one would see that lower dispersions of less correlated inputs are represented in the upper part of the black region and bigger dispersions in the lower part. The vertical stripes, which appear in the black region in the diagram, occur as a consequence of the finite sampling of parameter 2 (dispersion in the more correlated input group).

At a BP-spike shift T_{BP} of -5 ms a transition in the weight development occurs, where most of the time weights do neither grow nor shrink in both, the correlated and less correlated, groups. This transition has been made visible in the diagram by coloring BP-spike shifts between -5 ms and 5 ms in green. The reason for this type of behavior is that the BP-spike, being very close to the D-spike, overrules in these cases the effect of the D-spike. The randomness, whether the BP-spike comes causal or acausal to an individual synapse, is large enough in both, correlated and less correlated, groups, and leads to an averaging-out of the weight changes. Some-

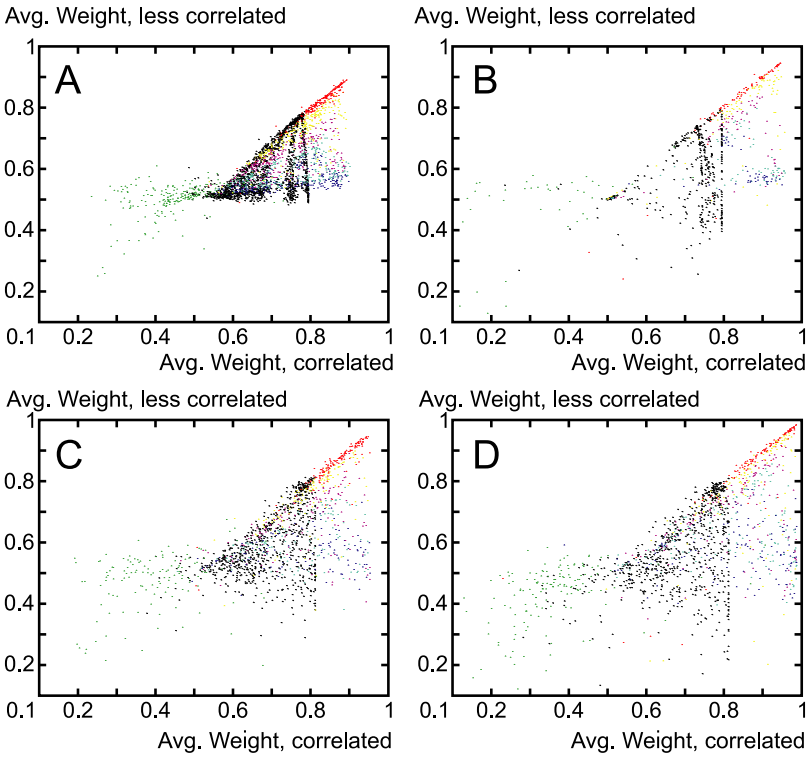

Fig. 9 Statistical parameter analysis. As in Fig. 8, plotted are the average weights of the less correlated group (ordinate) against the correlated group (abscissa). Colors depict different plasticity characteristics. Original parameter used in Fig. 8 were: AMPA $\tau = 6$ ms, NMDA $\tau = 117$ ms, D-spike $\tau = 235$ ms, BP-spike $\tau = 6$–66 ms, $q_1 = 0.14$, D-/BP-spike amplitude relation from $1/1.5$ to $1/15$, depending on BP-spike width, and keeping the area under the BP-spike constant, $\mu = 0.09$, first phase 200 pulse groups, second phase 400 pulse groups. Changed parameters in this fig. are now: (A) half of the BP-spike amplitude used in Fig. 8; (B) 100 simulated inputs in each group instead of three (threshold $q_1 = 2.4$). (C) faster learning rate $\mu = 1.5$, and 20 pulse groups first, 20 pulse group second phase, (D) the same as (C), but the second learning phase sets in at once, lasting 40 pulse groups

times also weight shrinkage is found in these cases probably as a consequence of the larger LTD-part in the STDP-curves.

It is probably reasonable to consider the green region with more general caution, too. In the model, the starting point of each signal (time point $t = 0$) can be well defined. In physiology, this time point is less obvious. Hence, close to the zero time point in the model actual physiological results may vary rather strongly like suggested by the rapid transition between LTP and LTD which occurs at this time point in the STDP-curves. Hence, black and colorful regions represent in our model the zone where results are clearly robust against this contingency, whereas green points may in reality sometimes "jump" into another domain in individual situations.

The remaining colors encode the dispersion of the wide, less correlated spike distributions in the case when time shifts of the BP-spike are positive (>5 ms, hence BP-spike after D-spike). Note, the black (less than −5 ms) and red-to-blue colored dots (more than +5 ms) overlay each other and at a BP-spike shift T_{BP} of +5 ms we find ourselves again on the left side of the black region. Dispersions are getting wider essentially from top to bottom (red to blue).

Multiple regions (from yellow to blue) show a transition from almost equal weight growth (diagonal tail) to asymmetric weight growth (horizontal tail). The exact location of this transition depends on the BP-spike shift T_{BP}.

The circle in the figure shows for the yellow (21–40 ms) or purple (41–60 ms) dots how the different BP-spike shifts T_{BP} are roughly represented in the figure. The diagonal tail develops from left to right for BP-spike shifts from about $T_{BP} = 80$ ms down to $T_{BP} = 30$–40 ms. Then data points drop until they reach the horizontal tail for about $T_{BP} = 20$ ms. Even smaller BP-spike shifts are represented towards the left side of the horizontal part of the curve.

Why are these changes arranged on a circle? For large BP-spike shifts, the BP-spike has little influence and both groups grow by the DS-mechanisms. If correlated and less correlated dispersions are similar, weights will grow in the same way (red, 1–20 ms), if the less correlated group has a wider dispersion, its weights will grow less (dark blue, 81–100 ms). As soon as the BP-spike gets closer to the D-spike, it will start to exert its influence. But this will first affect the less correlated group as there are almost always some inputs so late that they "collide" with the BP-spike. Time of collision, however, is random and sometimes these input are "pre" while sometimes they are "post" with respect to the BP-spike. Hence LTP and LTD will be essentially balanced

in the less correlated group, leading on average to zero weight growth. This effect is of course very pronounced when the less correlated group has a wide dispersion (blue, 81–100 ms), while it does not occur if the dispersion of correlated and less correlated groups are similar (red, 1–20 ms).

This also explains the not-shown inner structure of the black region (less than −5 ms), only here, negative BP-spike shifts $T_{BP} < 0$ lead to STDP curves with a dominance of the LTD part leading in many cases to weight shrinkage below zero.

The structure presented in Fig. 8 is not very sensitive to the BP-spike amplitude, as could be expected because the amplitude influences the function $\Delta\rho(T, T_{bp})$ linearly. In part A of Fig. 9 the same diagram obtained with a BP-spike with half amplitude is shown. In this case the general pattern persists, though the transitions to the lower tail of yellow or purple points are less pronounced.

The structure in Fig. 8, 9 is valid for a wide range of thresholds. To obtain the figures a threshold value $q_1 = 0.14$ was used. Similar distributions of colored clusters were obtained with thresholds in the interval [0.07, 0.2]. Below 0.07 the trivial case occurs, where a single spike is enough to pass threshold. Whereas beyond 0.2, passing the threshold became very rare, with almost no weight growth happening in the system.

In part B of Fig. 9 we show a plot of 1000 experiments performed with an original amplitude but with 100 inputs in each cluster (all threshold parameters were scaled accordingly), leading to the similar pattern. This shows that the results from the much higher number of experiments performed in the simplified model with less inputs can be trusted.

In part C we show a plot of 1500 experiments performed with much higher learning rate $\mu = 1.5$ and, consequentially, fewer iterations. In this situation the pre-growth phase is soon replaced by the fast-growth phase and noise-induced symmetry breaking effects play a stronger role. As a consequence the diagram, while still preserving the main features of panel A, becomes more diffuse and the horizontal tail begins to vanish. Many more "wrong" growth cases occur, too, similar to those in Fig. 6, leading to this increased dispersion. This effect becomes even more pronounced when we remove the pre-growth phase altogether in panel D of Fig. 9. All other parameter are like in C and now the diagram has lost most of its features, only the diagonal tail remains for clear-cut parameter combinations.

Finally it is interesting to relate these results to the analytical solutions provided above. The lines and arrows in Fig. 3(B) indicate what happens. The BP-spike shift, encoded by the different colors in Figs. 8, 9 is represented by the location of the black dot, which may shift along the x-axis (double arrow at the bottom). Colors black and green in Figs. 8, 9 relate to negative shifts in Fig. 3(B). The integration interval (brackets in Fig. 3(B)) depends on the degree of "correlatedness" of the inputs. It is smaller for the correlated group in Figs. 8, 9 and wider for the less-correlated group.

Acknowledgments The authors acknowledge the support from SHEFC INCITE as well as EU PACO-PLUS to F.W. and IBRO to M.T. We are grateful to B. Graham, L. Smith and D. Sterratt for their helpful comments on this manuscript. The authors wish to especially express their thanks to A. Saudargiene for her help at many stages in this project.

References

Abarbanel HDI, Gibb L, Huerta R, Rabinovich MI (2003) Biophysical model of synaptic plasticity dynamics. Biol. Cybern. 89(3): 214–226.

Abarbanel HDI, Huerta R, Rabinovich MI (2002) Dynamical model of long-term synaptic plasticity. Proc. Natl. Acad. Sci. (USA) 99(15): 10132–10137.

Bender VA, Feldman DE (2006) A dynamic spatial gradient of hebbian learning in dendrites. Neuron 51(2): 153–155 Commentary

Bi G-Q, Poo M (2001) Synaptic modification by correlated activity: Hebb's postulate revisited. Annu. Rev. Neurosci. 24: 139–166.

Bi GQ, Poo MM (1998) Synaptic modifications in cultured hippocampal neurons: dependence on spike timing, synaptic strength, and postsynaptic cell type. J. Neurosci. 18: 10464–10472.

Bliss TV, Gardner-Edwin AR (1973) Long-lasting potentiation of synaptic transmission in the dentate area of the unanaesthetized rabbit following stimulation of the perforant path. J. Physiol. (Lond.) 232: 357–374.

Castellani GC, Quinlan EM, Cooper LN, Shouval HZ (2001) A biophysical model of bidirectional synaptic plasticity: dependence on AMPA and NMDA receptors. Proc. Natl. Acad. Sci. (USA) 98(22): 12772–12777.

Eurich CW, Pawelzik K, Ernst U, Cowan JD, Milton JG (1999) Dynamics of self-organized delay adaptation. Phys. Rev. Lett. 82: 1594–1597.

Froemke RC, Dan Y (2002) Spike-timing-dependent synaptic modification induced by natural spike trains. Nature 416: 433–438.

Froemke RC, Poo M-m, Dan Y (2005) Spike-timing-dependent synaptic plasticity depends on dendritic location. Nature 434: 221–225.

Gasparini S, Migliore M, Magee JC (2004) On the initiation and propagation of dendritic spikes in CA1 pyramidal neurons. J. Neurosci. 24(49): 11046–11056.

Golding N, Kath WL, Spruston N (2001) Dichotomy of action-potential backpropagation in ca1 pyramidal neuron dendrites. J Neurophysiol. 86: 2998–3010.

Golding NL, Spruston N (1998) Dendritic sodium spikes are variable triggers of axonal action potentials in hippocampal CA1 pyramidal neurons. Neuron 21: 1189–1200.

Golding NL, Staff PN, Spurston N (2002) Dendritic spikes as a mechanism for cooperative long-term potentiation. Nature 418: 326–331.

Govindarajan A, Kelleher RJ, Tonegawa S (2006) A clustered plasticity model of long-term memory engrams. Nature Rev. Neurosci. (Perspectives) 7: 575–583.

Hebb DO (1949) The Organization of Behavior: A Neurophychological Study. Wiley-Interscience, New York.

Holthoff K (2004) Regenerative dendritic spikes and synaptic plasticity. Curr. Neurovasc. Res. 1(4): 381–387.

Holthoff K, Kovalchuk Y, Yuste R, Konnerth A (2004) Single-shock LTD by local dendritic spikes in pyramidal neurons of mouse visual cortex. J. Physiol. 560.1: 27–36.

Holthoff K, Kovalchuk Y, Yuste R, Konnerth A (2005) Single-shock plasticity induced by local dendritic spikes. In Proceedings of the Göttingen NWG Conference, p. 245B.

Karmarkar UR, Buonomano DV (2002) A model of spike-timing dependent plasticity: one or two coincidence detectors? J. Neurophysiol. 88: 507–513.

Karmarkar UR, Najarian MT, Buonomano DV (2002) Mechanisms and significance of spike-timing dependent plasticity. Biol. Cybern. 87: 373–382.

Kempter R, Gerstner W, van Hemmen JL (1999) Hebbian learning and spiking neurons. Phys. Rev. E. 59: 4498–4515.

Koch C (1999) Biophysics of Computation. Oxford University Press.

Larkum ME, Zhu JJ, Sakmann B (2001) Dendritic mechanisms underlying the coupling of the dendritic with the axonal action potential initiation zone of adult rat layer 5 pyramidal neurons. J. Physiol. (Lond.) 533: 447–466.

Letzkus JJ, Kampa BM, Stuart GJ (2006) Learning rules for spike timing-dependent plasticity depend on dendritic synapse location. J. Neurosci. 26(41): 10420–10429.

Magee JC, Johnston D (1997) A synaptically controlled, associative signal for Hebbian plasticity in hippocampal neurons. Science 275: 209–213.

Malenka RC, Nicoll RA (1999) Long-term potentiation-a decade of progress? Science 285: 1870–1874.

Markram H, Lübke J, Frotscher M, Sakmann B (1997) Regulation of synaptic efficacy by coincidence of postsynaptic APs and EPSPs. Science 275: 213–215.

Polsky A, Mel BW, Schiller J (2004) Computational subunits in thin dendrites of pyramidal cells. Nat Neurosci 7(6): 621–627.

Porr B, Wörgötter F (2003) Isotropic sequence order learning. Neural Comp. 15: 831–864

Rubin JE, Gerkin RC, Bi GQ, C CC (2005) Calcium time course as a signal for spike-timing dependent plasticity. J. Neurophysiol. 0–0.

Saudargiene A, Porr B, Wörgötter F (2004) How the shape of pre- and postsynaptic signals can influence STDP: a biophysical model. Neural Comp. 16: 595–626.

Saudargiene A, Porr B, Wörgötter F (2005a) Local learning rules: predicted influence of dendritic location on synapticmodification in spike-timing-dependent plasticity. Biol. Cybern. 92: 128–138.

Saudargiene A, Porr B, Wörgötter F (2005b) Synaptic modifications depend on synapse location and activity: a biophysical model of STDP. Biosystems 79: 3–10.

Senn W, Markram H, Tsodyks M (2000) An algorithm for modifying neurotransmitter release probability based on pre-and postsynaptic spike timing. Neural Comp. 13: 35–67.

Shouval HZ, Bear MF, Cooper LN (2002) A unified model of NMDA receptor-dependent bidirectional synaptic plasticity. Proc. Natl. Acad. Sci. (USA) 99(16): 10831–10836.

Shouval HZ, Kalantziz G (2005) Stochastic properties of synaptic transmission affect the shape of spike time-dependent plasticity curves. J. Neurophysiol. 93: 1069–1073.

Sjöström PJ, Häusser M (2006) A cooperative switch determines the sign of synaptic plasticity in distal dendrites of neocortical pyramidal neurons. Neuron 51(2): 227–238.

Song S, Miller KD, Abbott LF (2000) Competitive hebbian learning through spike-timing-dependent synaptic plasticity. Nature Neurosci. 3: 919–926.

Stuart G, Spruston N, Sakmann B, Häusser M (1997) Action potential initiation and backpropagation in neurons of the mammalian central nervous system. Trends Neurosci. 20: 125–131.

Swindale NV (1996) The development of topography in the visual cortex: a review of models. Network 7(2): 161–247.

Wang H-X, C GR, Nauen DW, Bi G-Q (2005) Coactivation and timing-dependent integration of synaptic potentiation and depression. Nature Neurosci. 8: 187–193.

Wespatat V, Tennigkeit F, Singer W (2004) Hebbian plasticity rules in fast oscillating visual cortical cells. In: FENS Forum Abstracts, FENS Lisbon, vol. 2, p. A031.2.

Williams SR, Stuart GJ (2003) Role of dendritic synapse location in the control of action potential output. TINS 26(3): 147–154.

Yeung LC, Shouval HZ, Blais BS, Cooper LN (2004) Synaptic homeostasis and input selectivity follow from a calcium-dependent plasticity model. Proc. Natl. Acad. Sci. 101: 14943–14948.